

Activated Carbon Derived From OPEFB by One Step Steam Activation and Its Application for Dye Adsorption: Kinetics and Isothermal Studies

Fahriya Puspita Sari ^{1*}, Dede Heri Yuli Yanto ¹⁾, and Gustan Pari ³⁾

¹⁾ Research Center for Biomaterials, Indonesian Institute of Sciences
Jl. Raya Bogor, KM 46, Cibinong, Bogor, Indonesia

²⁾ Forest Products Research and Development Center,
Ministry of Environment and Forestry Republic of Indonesia
JL. Gunung Batu No. 5 Bogor, Indonesia

*) Corresponding author: fahriya.ps07@gmail.com

(Received: March 14, 2019 Accepted: July 03, 2019)

Abstract

Activated carbon was prepared from OPEFB by one step steam activation method. The adsorption performance for the removal of acid orange 52 (AO 52), reactive blue 19 (RB 19), basic violet 1 (BV 1) was investigated. Each dye has a different chemical structure such as azoic, anthraquinone, triarylmethane for AO 52, RB 19, and BV 1 respectively. The effects of adsorbent dosage, pH, and contact time on the adsorption process were studied. Experimental data were analyzed by model equations such as Langmuir, Freundlich and Temkin isotherms and it was found that the Langmuir isotherm model best fitted for all three dyes with R² values is higher than 0.95. Langmuir model assumes a homogeneous nature and monolayer coverage of dye molecules at the outer surface of activated carbon. Adsorption kinetics was determined using pseudo-first-order, pseudo-second-order rate equations, Elovich model and also intraparticle diffusion models. Kinetic studies showed that the pseudo-second-order kinetic model better described the adsorption process with R² values exceeds 0,99 compared with the other kinetics model. The SEM images showed AC pores was well developed with steam activation while wider porosity is created in the macropore range. FT-IR analysis had shown that the AC functional groups were disappeared because of vaporization the volatile materials when the heating process.

Keywords: Activated Carbon, Adsorption Isotherms, Kinetic, OPEFB, Steam Activation

How to Cite This Article: Sari, F.P., Yanto, D.H.Y., and Pari, G. (2019), Activated Carbon Derived From OPEFB by One Step Steam Activation and Its Application for Dye Adsorption: Kinetics and Isothermal Studies, Reaktor, 19(2), 68-76, <http://dx.doi.org/10.14710/reaktor.19.02.68-76>.

INTRODUCTION

Wastewater treatment using adsorption techniques has been widely used for removing pollutant because of their efficiency in treating waste

which is difficult with biological treatment. One of the most popular adsorbents now days is activated carbon (Kyzas et al., 2013). Activated carbon has a large porous surface area, high adsorption capacity and rate,

thermostability and low acid/base reactivity and specific surface reactivity (Kyzas et al., 2013)(Kılıç et al., 2012)(Li et al., 2010). All the advantage makes activated carbon very effective and becomes an ideal alternative to remove various types of dyes.

Dye-containing effluents from the textile and leather industries can cause various environmental impacts, due to their hazardous effect. Toxicity and carcinogenic aspects are occurred by the reductive cleavage of azo groups in the chemical structure of dyes (Akar et al., 2015). Dyes may be classified in several ways, according to the chemical constitution, application class, and end use. Dyes are now classified according to how they are used in the dyeing process. The presence of a chromophore group provides the color of a dye. A chromophore group is a radical configuration consisting of conjugated double bonds as azo, nitro, methine, anthraquinone, triarylmethane, indigo, phtalocyanine (Allen & Koumanova, 2005)(Gürses et al., 2016). Main dyes are grouped as acid dyes, basic dyes, direct dyes, mordant dyes, vat dyes, reactive dyes, disperse dyes, azo dyes, and sulfur dyes (Demirbas, 2009).

In this research, we prepared activation by physical activation with steam. The procedure of steam activation can be regarded as a simple, environmentally friendly approach, cheaper, and produce activated carbon with well-developed pore structure and good physical strength (Fu et al., 2013)(Amosa et al., 2014)(Rashidi & Yusup, 2016). Chemical activation has the ability to form high specific surface area and highly developed porous structures. However, a large amount of chemical agents would be consumed during the chemical activation process, which could generate wastewater and bring about the secondary pollution and the process of preparation is relatively complex (Prauchner & Rodríguez-Reinoso, 2012). Steam activation needs a lower temperature than CO₂ activation due to its higher reactivity. Steam-activated carbon also has higher surface area because the steam

molecules are smaller in size than CO₂ and hence, are easily diffused and reacted with carbon to develop the porosity (Rashidi & Yusup, 2016).

In this work, OPEB used as the precursor of activated carbon by steam activation. The effect of adsorbent dosage, pH, reaction contact time, and initial dyes concentration on the adsorption efficiency of acid orange 52, reactive blue 19, and basic violet 1 dyes was investigated. The adsorption kinetic studies were performed using the pseudo-first, pseudo-second-order models and Elovic equation. Freundlich, Langmuir, Temkin isotherm models were used to study the adsorption equilibrium. Functional and surface characterization of the prepared adsorbent was performed.

MATERIALS AND METHODS

Materials

Oil palm empty fruit bunch used as the precursor of activated carbon was provided from oil palm plantation in Sukabumi, West Java Province, Indonesia. First, OPEFB were crushed and sieved into particles of 5-10 mesh and then washed and dried at 60°C for about 48 h. Acid orange 52 (AO 52), an azo dye, (empirical formula is C₁₄H₁₄N₃NaO₃S and MW = 327.33 g mol⁻¹), reactive blue 19 (RB 19), an anthraquinone dye, (empirical formula is C₂₂H₁₆N₂Na₂O₁₁S₃ and MW = 626.54 g mol⁻¹) and basic violet 1 (BV 1), a triarylmethane dye, (empirical formula is C₂₄H₂₈ClN₃ and MW = 393.95 g mol⁻¹) were supplied by Sigma Aldrich. The chemical structure of AO 52, RB 19, BV 1 is shown in Figure 1.

Methods

Preparation of activated carbon

Activated carbon samples are prepared by carbonization and activation of OPEB by one step process. 100 gr of OPEB materials are loaded in the horizontal tubular furnace and then carbonated at 700°C.

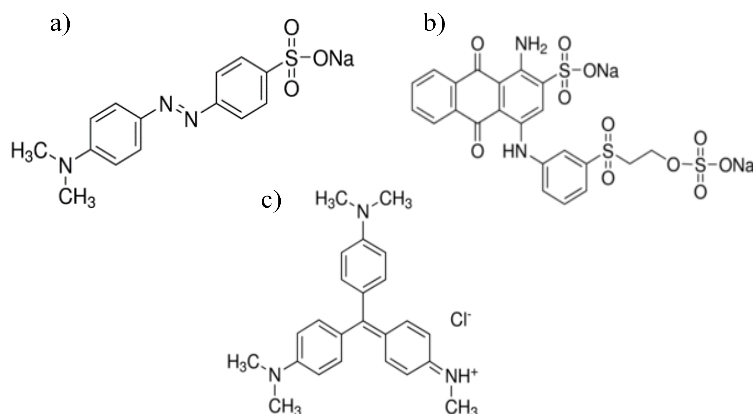


Figure 1. Chemical Structure of a) Acid Orange (azoic structure), b) Reactive Blue 19 (anthraquinone structure), and c) Basic Violet 1 (triarylmethane structure)

Once the temperature was reached at 700°C, the materials are activated with steam and maintained for 1 hour, the steam flow rate of 5 ml/min and steam pressure of 100 ml bar. The products are cooled to room temperature and then ground and sieved until particle size lower than 90µm.

Characterization

The morphology of activated carbon produced from OPEFB and saturated activated carbon by AO 52, RB 19, and BV 1 was examined using scanning electron microscopy (Keyence VE-9800). Chemical characterization was carried out by attenuated total reflectance (ATR)-FTIR using FTIR Perkin Elmer two spectrum in the wavelength range of 4000-400 cm⁻¹ to identify the functional groups at the surface of carbon materials.

Analytical measurements

The unknown concentration of dyes was determined by finding out the absorbance at the characterization wavelength using double beam UV/Visible spectrophotometer (Hitachi U-2001). Standard curve chart was prepared by measuring the absorbance of difference dye concentration (100-1000 ppm) at 505 nm for AO 52, 592 nm for RB 19, and 584 nm for BV 1.

Effect of pH, adsorbent dosage, and contact time

The effect of pH on dye removal was tested by varying the pH from 3-11, with initial dye concentration of 500 mg/L, activated carbon dosage of 15 mg/20 ml and adsorption temperature of 30°C for 24 h. The initial pH was adjusted by addition of HCl or NaOH aqueous solution. The effect of variation of mass of carbon was studied by increasing the activated carbon dosage from 15 mg/20 mL to 75 mg/20 mL with the same temperature and contact time. The influence of contact time was assessed by using the same dye concentration and changing the contact time from 15-300 min. The amount adsorbed per unit mass of activated carbon (mg/g) is calculated using the following equation (1):

$$q_t = \frac{(C_0 - C_t)V}{W} \quad (1)$$

where C_0 and C_t (mg/L) are the liquid-phase concentrations of dye at initial and time (t), respectively. V (L) is the volume of the solution, and W (g) is the mass of adsorbent used.

Equilibrium experiments

The batch adsorption experiments were undertaken in Erlenmeyer flasks containing 15 mg of adsorbent and equal volumes (20 mL) of dyes solutions (AO 52 and RB 19) at varying concentrations (300–700 mg/L). The flask was kept at 30°C with an agitation speed of 120 rpm for 24 h. The dye concentrations in the supernatant were analyzed

UV-vis spectrophotometer. Each experiment was duplicated under identical conditions. Dyes uptake at equilibrium, q_e (mg/g), was calculated by equation (2):

$$q_e = \frac{(C_0 - C_e)V}{W} \quad (2)$$

where C_0 and C_e (mg/L) are the liquid-phase concentrations of dye at initial and equilibrium, respectively. V (L) is the volume of the solution, and W (g) is the mass of adsorbent used.

RESULTS AND DISCUSSIONS

Effect of adsorbent dosage

The effect of activated carbon (AC) dosage (15-75 mg/20 mL) on the decolorization percentage and adsorption capacity of 3 types of dyes was studied using 500 mg/L of dyes concentration. Fig 2. shows the result of decolorization percentage from AO 52, RB 19, and BV 1.

The decolorization increased with increase in AC dosage until a constant value was achieved. Decolorization percentage of AO 52 continues to increase until AC dosage is 75 mg with 94.25 %. It was different with the other dyes (RB 19 and BV 1), RB 19 decolorization continue to increase until AC adsorbent is 45 mg and became constant until 75 mg with maximum decolorization is 97.07%. BV 1 decolorization continue to increase until AC adsorbent is 60 mg and became constant until 75 mg with maximum decolorization is 92.96%. Thus, it can be explained that increasing the AC dosage cause the availability of the active site for dyes adsorption increases.

The adsorption ability may be distinguished by the dye structure and chemical functional groups. Molecular weight of AO 52 < BV 1 < RB 19.

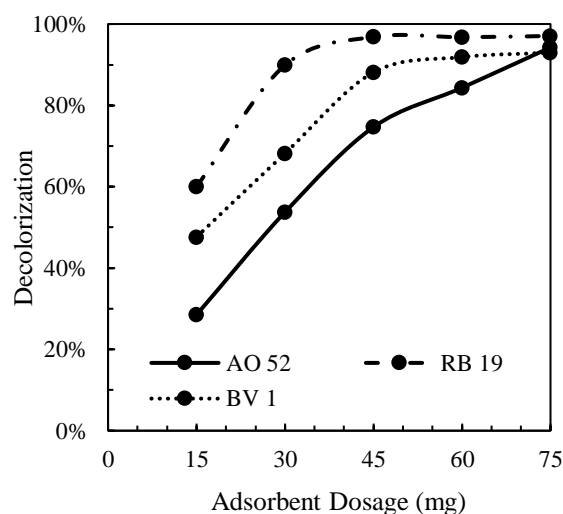


Figure 2. Effect of adsorbent dosage in the adsorption of AO 52, RB 19, and BV 1 with initial dye concentration of 500 mg/L

Effect of Solution pH

The initial pH of solution could significantly influence the adsorption process. Fig 3. shows the variation in the decolorization of dyes at various system pH. It was evident that the maximum decolorization of AO 52 is observed at pH 3, RB 19 and BV 1 at pH 11. Under the neutral and alkaline condition, the change of initial pH had no significant effect on the adsorption for AO 52 into AC.

It was found that optimum decolorization of AO 52 is 80.52% at pH 3, at higher pH decolorization of AO 52 remaining constant until pH 11. In contrast with RB 19 and BV 1, decolorization increase until pH maximum. At pH 3, decolorization of RB is 36.89% and increase until 51.48% at pH 5, decolorization become constant at pH 5-9 and increase again in pH 11. For BV 1, decolorization increase significantly from pH range 5-11 until decolorization reach 91.46%.

Effect of contact time

One of the important parameters for the adsorption process is contact time. Optimization of contact time in the adsorption process is necessary to develop cost-effective procedure (Maneerung et al., 2016). Fig 4. shows the time course of the adsorption of AO 52, RB 19, and BV 1. It can be observed that the uptake of the dye increased with time and, at some point in time, reached a constant value where no more dyes were removed. For an initial concentration of 500 mg/L, the percentage decolorization increase with time and become constant thereafter. For AO 52 and RB 19, the percentage of decolorization increases rapidly for 60 min and the increase become gradual thereafter. The dyes adsorption are 27.99% and 46.85% for AO 52 and RB 19, respectively. Whereas, the percentage decolorization of BV 1 increase rapidly for 180 min and still increase until 300 min until the adsorption of the dye is 42.3%.

This phenomenon implied the availability of readily accessible surface sites at the initial stage, which is due to the high vacant sites of the activated carbon for the adsorption and gradually decreased as equilibrium approached which is due to the saturation of the active sites for the adsorption.

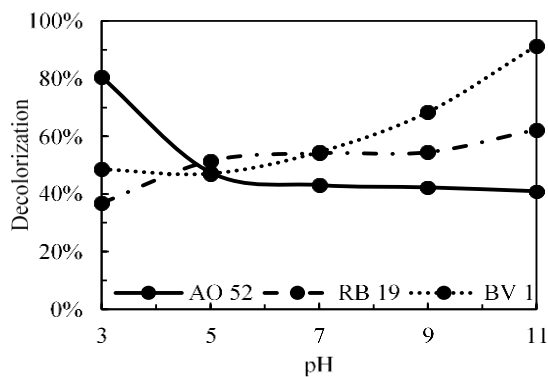


Figure 3. Effect of solution pH in the adsorption of AO 52, RB 19, and BV 1 with initial dye concentration of 500 mg/L

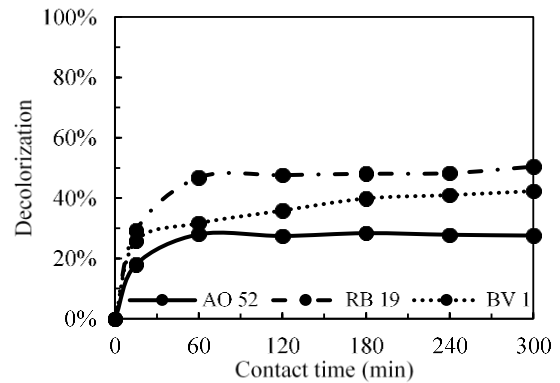


Figure 4. Effect of contact time in the adsorption of AO 52, RB 19, and BV 1 with initial dye concentration of 500 mg/L

Adsorption isotherm model

The adsorption isotherm is used to define the characteristic of the adsorption process between liquid and solid phases when it reaches the equilibrium state. Thus the adsorption isotherm study was carried out. Adsorption isotherm provides an insight into both mechanism and interaction between the adsorbent surfaces. The Langmuir, Freundlich, and Temkin models were selected to fit the equilibrium. These isotherms are usually performed by fixing the mass of adsorbent while changing the concentration of the adsorbate in an appropriate range (Maneerung et al., 2016)(Foo & Hameed, 2011)(Heibati et al., 2015). Data obtained from the batch adsorption experiments by varying the initial concentration of AO 52, RB 19, and BV 1 ranging from 300 to 700 mg/L. Table 1 shows the equation of adsorption of three isotherm model (Langmuir, Freundlich, and Temkin equation) and the linearized form to find out isotherm parameters.

Table 2 shows the isotherm model for AO 52, RB 19, and BV 1. Langmuir isotherm model is the best fit for all 3 dyes with R2 values is higher than 0.95. From experimental data to the isotherm model (predicted value) are according to the following order; Langmuir > Freundlich > Temkin. Langmuir model assumes a homogeneous nature and monolayer coverage of dye molecules at the outer surface of activated carbon. Thus once a dye molecule is adsorbed, it will occupy the AC site, and no further adsorption can take place at that particular active site. Hence, a maximum adsorption capacity will occur where no more adsorption will happen.

Adsorption kinetics

The kinetics of adsorption describes the rate of adsorbate uptake on the adsorbent, and it controls the efficiency of the process and the equilibrium time. The kinetic parameters are helpful for the prediction of adsorption rate, which gives important pieces of information for designing and modeling the processes, in order to determine the adsorption mechanism and the potential rate-limiting steps (Ahmed, 2016)(Chen

et al., 2010). Four kinetics model : pseudo-first order (Lagergren, 1898), pseudo-second order (Ho & McKay, 1999), Elovich (Aharoni & Tompkins, 1970) , intra-particle diffusion (Weber & Morris, 1963) (Fig 4) used to correlate the experimental kinetics data of

AO 52, RB 19, and BV 1 on activated carbon. Table 2 showed the results fit well correlation of experimental data by a pseudo-second-order kinetic model with R2 values exceeds 0.99 compared with the other kinetics model.

Table 1. Equation of adsorption isotherm model

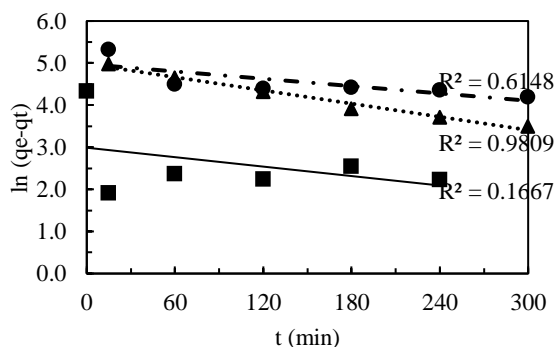
Adsorption Isotherm Model	Equation	Linearized form
Langmuir Equation	$q_e = \frac{Q_L K_L C_e}{1 + K_L C_e}$	$\frac{1}{q_e} = \frac{1}{Q_L} + \frac{1}{K_L Q_L C_e}$
Freundlich Equation	$q_e = K_f C_e^{1/n}$	$\ln q_e = \ln K_f + \frac{1}{n} \ln C_e$
Temkin Equation	$q_e = B \ln(A C_e)$	$q_e = B \ln A + B \ln C_e$

where QL (mg/g) and KL (L/g) are Langmuir constants related to adsorption capacity and adsorption energy, and KF (mg/g).(L/mg)^{1/n} and 1/n are Freundlich adsorption constant and a measure of adsorption intensity. B = RT/b, with b (J/mol), A (L/g), R (8.314 J/mol K) and T (K) are the Temkin constant related to the heat of sorption, equilibrium binding constant, gas constant and absolute temperature

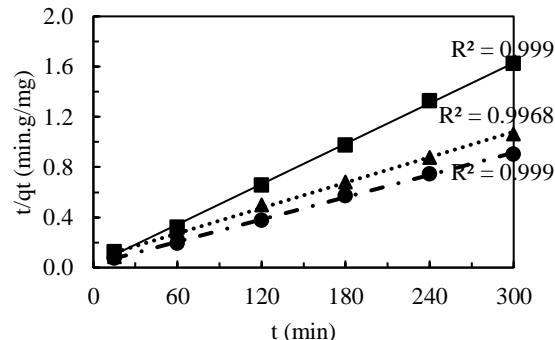
Table 2. Isotherm parameters for the adsorption of AO 52, RB 19, and BV 1 at 303K onto activated carbon

Isotherm Model	Parameter	AO 52	RB 19	BV 1
Langmuir	QL	196.08	204.08	588.24
	KL	0.009	0.029	0.004
	R ²	0.958	0.998	0.954
Freundlich	K _f	1.199	103.97	16.65
	1/n	0.181	0.098	0.517
	R ²	0.651	0.911	0.948
Temkin	A	0.611	93.178	0.03
	B	27.88	17.72	145.86
	R ²	0.642	0.908	0.945

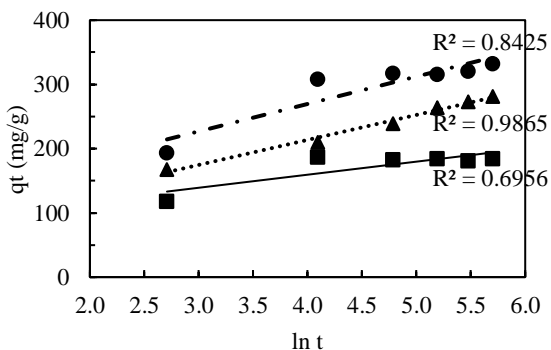
(a) Pseudo orde 1



(b) Pseudo Orde 2



(c) Elovich



(d) Intraparticle Diffusion

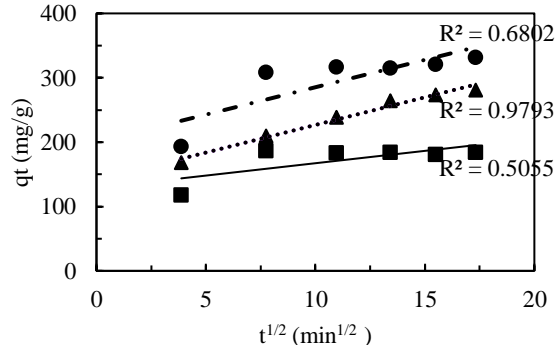


Figure 5. Adsorption kinetics plot : (a) pseudo orde1, (b) pseudo orde 2, (c) elovich, (d) intraparticle diffusion, for the adsorption of AO 52, RB 19, and BV 1

Table 3 Kinetics of isotherm constants and regression correlation coefficients for the adsorption of AO 52, Rb 19, BV 1 onto activated carbon.

Kinetics Model	Equation Form	Parameter	AO 52	RB 19	BV 1
		qe(exp)	184,4	332,1	281.3
Pseudo orde 1	$\ln(q_t - q_e) = \ln(q_e) - K_1 t$	Qe	25.02	144.81	145.345
		k ₁	0.004	0.003	0.005
		R ²	0.251	0.615	0.981
Pseudo orde 2	$\frac{1}{q_t} = \frac{1}{K_2 q_e} + \frac{1}{q_e}$	Qe	185.12	333.33	294.118
		k ₂	0.0013	0.0003	1.7.E-04
		R ²	0.999	0.999	0.997
Elovich	$q_t = \frac{1}{b} \ln(axb) + \frac{1}{b} \ln(t)$	A	955.78	432.5	171.219
		B	0.049	0.0234	0.026
		R ²	0.696	0.843	0.987
Intraparticle diffusion	$q_t = K_2 t^{1/2} + C$	k _{id}	3.84	8.5023	8.587
		C	128.84	200.27	140.830
		R ²	0.506	0.680	0.979

Pseudo-second order model suggested that the rate-controlling step is chemisorption involving valence forces through the exchange or sharing of electrons between the adsorbate molecules and the surface functional groups of the adsorbent.

The pseudo-second-order kinetic parameters obtained could be used to determine the equilibrium sorption capacity, percentage of the removal of dyes, rate constants and initial sorption rate for a bioreactor design (Chen et al., 2010). Elovich kinetic equation is one of the most useful models describing chemisorptions processes (Foo & Hamed, 2012). The intra-particle diffusion model is widely used to predict the rate controlling step, which mainly depends on either surface or pore diffusion (Abbas & Ahmed, 2016). R2 value (Table 2) for this model is lower compared to those of pseudo-second order and Elovich models. From these results, it can be concluded that intra-particle diffusion is not the dominating mechanism for the dyes-activated carbon adsorption

system and that some other mechanism may play an important role during the adsorption

SEM and FTIR analysis

Fig 6 shows the scanning electron microscope (SEM) image of activated carbon before and after dyes adsorption. As seen in figure 6a, the pores are well developed with steam activation. It indicates that steam successfully diffused and reacted with carbon to develop and wider porosity is created. The pore development caused by steam activation is in the macropore range (pore size larger than 50 nm). Fig. 6b-d shows the activated carbon after the adsorption of the dye. It is clearly showed that the porous of activated carbon is already saturated with AO 52, RB 19, and BV 1. SEM-EDS analysis of activated carbon was used to characterize the elemental composition of the sample. According to SEM-EDS analysis, activated carbon consisted of 100% carbon and no other elements contained in the sample.

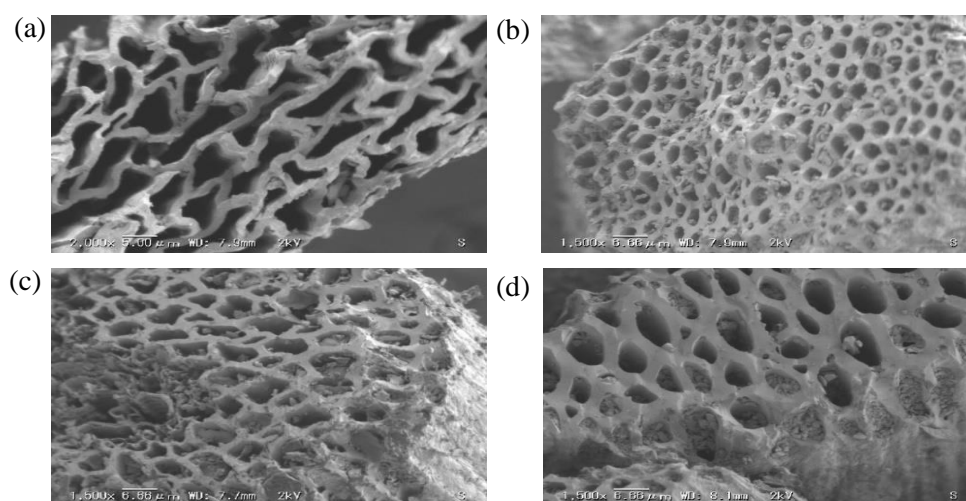


Figure 6. The SEM image of (a) activated carbon (AC), (b) AC + AO 52, (b) AC + RB 19, (c) (b) AC + BV

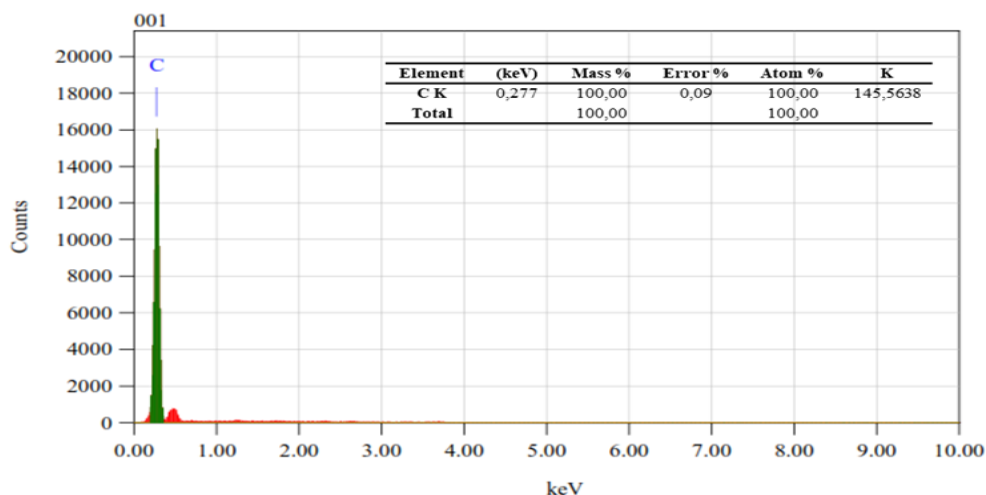


Figure 7. SEM-EDS analysis of activated carbon

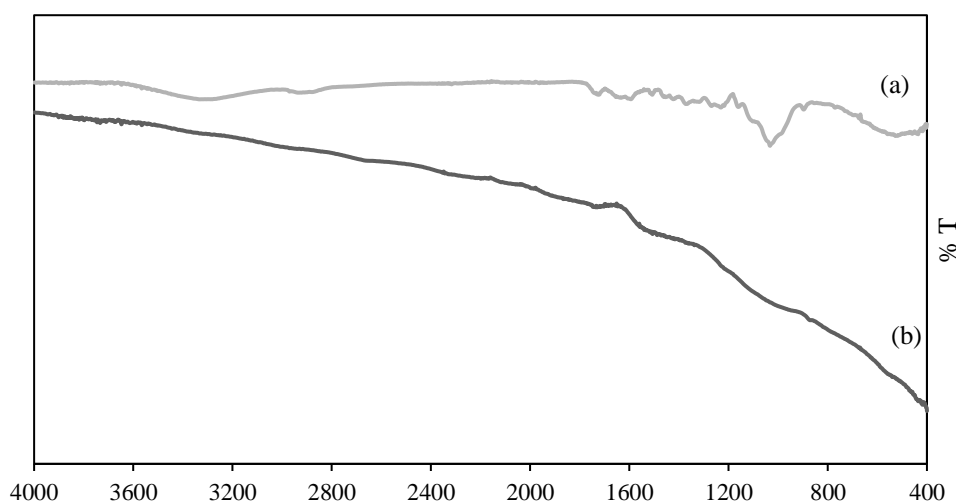


Figure 8. FTIR spectra of (a) raw material (OPEFB) and (b) activated carbon with steam activation

FTIR spectra were used to investigate the functional group presence in the raw material OPEFB and activated carbon. For raw material OPEFB (Fig. 8a), the area of 1800 cm^{-1} to 600 cm^{-1} is called the fingerprint area of spectra which has many sharp and well-defined absorption bands due to the various functional groups present in each component of OPEFB (Rosli *et al.*, 2017). The peak at around 1730 cm^{-1} can be seen from the spectra was corresponding to the C=O functional group. The peak at 1635 cm^{-1} corresponded to the bending vibration of the hydroxyl groups of cellulose. The bands at 1730 cm^{-1} was corresponding to the C=O functional group. The EFB sample also shows two important adsorption peaks at 1033 cm^{-1} which refers to the C-O stretching functional group. (Hidayu *et al.*, 2013). Fig 8b shows the FTIR spectra of activated carbon. It shows that most of the peaks of functional groups disappeared. This phenomenon is the same as FTIR analysis from Hidayu *et al.* (2013). Hidayu *et al.* (2013) reported that the functional groups from activated carbon

disappeared because the functional groups from the raw material spectrum were vaporized as volatile materials when the heat was supplied to the sample. The results obtained were in accordance with the FE-SEM analysis, and the activation process had been a success

CONCLUSIONS

Activated carbon from OPEFB by one step steam activation was proved to be an efficient process to adsorb AO 52, RB 19, BV 1. The decolorization increased with increase in AC dosage. Effect of solution pH showed that the maximum decolorization of AO 52 is observed at pH 3, RB 19 and BV 1 at pH 11. Adsorption of the uptake of the dye increased with time and at some point, of time reached a constant value which indicates that equilibrium had been approached. The kinetics of adsorption found that the adsorption process followed the pseudo-second-order model and Langmuir isotherms can well represent the adsorption isotherm.

ACKNOWLEDGEMENTS

The authors highly thank Research Center for Biomaterials LIPI and Forest Research and Development Center for facilitating laboratory and all the equipment to carry out this work

REFERENCES

Abbas, A.F. and Ahmed, M.J., 2016. Mesoporous activated carbon from date stones (*Phoenix dactylifera* L.) by one-step microwave assisted K₂CO₃ pyrolysis. *Journal of Water Process Engineering*, 9, pp.201-207.

Aharoni, C. and Tompkins, F.C., 1970. Kinetics of adsorption and desorption and the Elovich equation. *Advances in catalysis*, 21, pp.1-49.

Ahmed, M.J., 2016. Application of agricultural based activated carbons by microwave and conventional activations for basic dye adsorption. *Journal of Environmental Chemical Engineering*, 4(1), pp.89-99.

Akar, S.T., Yilmazer, D., Celik, S., Balk, Y.Y. and Akar, T., 2015. Effective biodecolorization potential of surface modified lignocellulosic industrial waste biomass. *Chemical engineering journal*, 259, pp.286-292.

Allen, S.J. and Koumanova, B., 2005. Decolourisation of water/wastewater using adsorption. *Journal of the University of Chemical Technology and Metallurgy*, 40(3), pp.175-192.

Amosa, M.K., Jami, M.S., Alkhatib, M., Jimat, D.N. and Muyibi, S.A., 2014. Comparative and optimization studies of adsorptive strengths of activated carbons produced from steam-and CO₂-activation for BPOME treatment. *Advances in Environmental Biology*, 8(3), pp.603-612.

Chen, S., Zhang, J., Zhang, C., Yue, Q., Li, Y. and Li, C., 2010. Equilibrium and kinetic studies of methyl orange and methyl violet adsorption on activated carbon derived from *Phragmites australis*. *Desalination*, 252(1-3), pp.149-156.

Demirbas, A., 2009. Agricultural based activated carbons for the removal of dyes from aqueous solutions: a review. *Journal of hazardous materials*, 167(1-3), pp.1-9.

Foo, K.Y. and Hameed, B.H., 2011. Preparation of oil palm (Elaeis) empty fruit bunch activated carbon by microwave-assisted KOH activation for the adsorption of methylene blue. *Desalination*, 275(1-3), pp.302-305.

Fu, K., Yue, Q., Gao, B., Sun, Y. and Zhu, L., 2013. Preparation, characterization and application of lignin-based activated carbon from black liquor lignin

by steam activation. *Chemical engineering journal*, 228, pp.1074-1082.

Gürses, A., Açıkıldız, M., Güneş, K. and Gürses, M.S., 2016. Dyes and pigments: their structure and properties. In *Dyes and Pigments* (pp. 13-29). Springer, Cham.

Heibati, B., Rodriguez-Couto, S., Al-Ghouti, M.A., Asif, M., Tyagi, I., Agarwal, S. and Gupta, V.K., 2015. Kinetics and thermodynamics of enhanced adsorption of the dye AR 18 using activated carbons prepared from walnut and poplar woods. *Journal of Molecular Liquids*, 208, pp.99-105.

Ho, Y.S. and McKay, G., 1999. Pseudo-second order model for sorption processes. *Process biochemistry*, 34(5), pp.451-465.

Kılıç, M., Apaydın-Varol, E. and Pütün, A.E., 2012. Preparation and surface characterization of activated carbons from *Euphorbia rigida* by chemical activation with ZnCl₂, K₂CO₃, NaOH and H₃PO₄. *Applied surface science*, 261, pp.247-254.

Kyzas, G.Z., Kostoglou, M., Lazaridis, N.K. and Bikiaris, D.N., 2013. Decolorization of Dyeing Wastewater Using Polymeric Absorbents-An Overview. In *Eco-Friendly Textile Dyeing and Finishing*. InTech.

Lagergren, S., 1898. Zur theorie der sogenannten adsorption gelöster stoffe. *Kungliga svenska vetenskapsakademiens. Handlingar*, 24, pp.1-39.

Li, K., Zheng, Z. and Li, Y., 2010. Characterization and lead adsorption properties of activated carbons prepared from cotton stalk by one-step H₃PO₄ activation. *Journal of hazardous materials*, 181(1-3), pp.440-447.

Maneerung, T., Liew, J., Dai, Y., Kawi, S., Chong, C. and Wang, C.H., 2016. Activated carbon derived from carbon residue from biomass gasification and its application for dye adsorption: kinetics, isotherms and thermodynamic studies. *Bioresource technology*, 200, pp.350-359.

Prauchner, M.J. and Rodríguez-Reinoso, F., 2012. Chemical versus physical activation of coconut shell: A comparative study. *Microporous and Mesoporous Materials*, 152, pp.163-171.

Rashidi, N.A. and Yusup, S., 2017. A review on recent technological advancement in the activated carbon production from oil palm wastes. *Chemical Engineering Journal*, 314, pp.277-290.

Rosli, N.S., Harun, S., Jahim, J.M. and Othaman, R., 2017. Chemical and physical characterization of oil

palm empty fruit bunch. *Malaysian Journal of Analytical Sciences*, 21(1), pp.188-196.

Weber, W.J. and Morris, J.C., 1963. Kinetics of adsorption on carbon from solution. *Journal of the Sanitary Engineering Division*, 89(2), pp.31-60.